Land Subsidence Monitoring in city area by Time Series Interferometric SAR Data

Huanyin Yue
Institute of Electronics, Chinese Academy of Sciences
No.19, Beisihuan Xilu, Haidian District, Beijing, P.R.China, 100080, Email: yuehuanyin@126.com
Huadong Guo, Quan Chen
Institute of Remote Sensing Applications, CAS
P.O.Box 9718, No.3, Datun Road, Chaoyang District, Beijing, P.R. China,100101

Ramon Hanssen, Freek van Leijen, Peter Marinkovic, Gini Ketelaar
Delft Institute of Earth Observation and Space Systems, Delft University of Technology, Kluyverweg 1, 2629 HS, Delft, the Netherlands
Email: R.F.Hanssen@lr.tudelft.nl

Abstract—**In this paper, the time series multi-image stack processing technique is implemented based on the ERS-1, ERS-2 SAR data set of cities of Las Vegas in America. A single master approach is used in the stack data processing based on the permanent scatterers processing technique invented by Ferretti et al. [1,2]. After the differential phase model establishment and stable points selection, linear subsidence velocity and digital elevation model errors are estimated, non-linear subsidence velocity and atmospheric artifacts related to each SAR acquisition are separated, so a land subsidence history covering all the SAR data acquisitions in each city can be achieved. In our research, more test data in cities of China will be implemented in the next step.**

Keywords-Land subsidence; time series InSAR data; phase model;

I. INTRODUCTION

Land subsidence occurs in many big cities all over the world, it has been a global problem. In the United states, more than 17,000 square miles in 45 states, have been directly affected by subsidence. The principal causes are aquifer-system compaction, drainage of organic soils, underground mining, hydrocompaction, matural compaction, sinkholes, and thawing permafrost [3]. In China, land subsidence happens in more than 50 cities of 16 provinces which are distributing at Yangtse river delta, Songliao and Huanghuai plain, southeast coastal plain, inland plain and basin as Xi'an, Taiyuan and Datong. The area of subsidence reaches 48655 km^2. It is a kind of serious geological disaster especially in the big cities, which can damage the buildings, bridges, roads, storm drains, canals and underground pipelines, cause changes in elevation and slope of streams, canals and drains, lead to the failure of well casings from forces generated by compaction of fine-grained materials in aquifer systems. In some coastal areas, subsidence has resulted in tides moving into low-lying areas that were previously above high-tide level.

Since monitoring the subsidence is a prerequisite to the relief of damage, it has been demonstrated that SAR interferometry is a powerful technology with a high potential land subsidence monitoring.

The advent of satellite or airborne radar interferometry (InSAR) in the early '90s [4], provided geometric information that significantly changed the perception and potential feasibility of deformation measurements [5]. This technique delivers spatially near-continuous deformation data, based on single repeated but instantaneous acquisitions, acquired systematically over the planet, including remote and inaccessible areas [6]. Monitoring of deformation depends on the availability of an archive of data (potential null-surveys) and does not need artificially installed benchmarks. Principal accuracies reach down to the mm-level [5].

Although InSAR has resulted in a revolution in deformation monitoring, its use can still be regarded as rather opportunistic because of the temporal and spatial decorrelation. Ferretti et al. [1,2] proposed a technique, called permanent scatterers processing, by using multi-temporal SAR data to estimate the interferometric phase of stable, point like scatterers and demonstrated that a large number of such scatterers can be detected in stacks of ERS SAR data in urban area. Although this technique overcomes the temporal and spatial decorrelation in some degree by exploring the interferometric phase information of some stable scatterers, especially some man made features in the urban area, a deformation evolution history in the time span of SAR data stack can be derived, it is still considered opportunistic due to the random and unpredictable selection and distribution of the stable scatterers within the SAR image, which depend on local condition of the earth surface and acquisition availability.

In this paper, we do some changes of this permanent scatterers technique, and use ERS SAR data stacks of Las Vegas to validate this algorithm. Test data in cities of China will be implemented in the next step of our research.

II. PHASE MODEL

In the interferometric SAR data processing, the interferograms are generated by combining two complex SAR images, the interferometric phase observation per resolution cell is composed by a number of contributors [5]:

$$\phi_{\text{int}} = \phi_{topo} + \phi_{defo} + \phi_{orb} + \phi_{atm} + \phi_{scat} + \phi_{noise} \quad (1)$$

where

ϕ_{int} : interferometric phase

This research is sponsored by the National Natural Science Foundation of China(40301032), KGW project, the digital Olympic game in Beijing and the Joint Research Project between China and the Netherlands

ϕ_{topo} : the topographic phase, which is a function of the wavelength λ , the perpendicular baseline $B_{\perp}$, the local incidence angle with respect to the reference ellipsoid α , and the slant range from the master platform to the earth surface *R*, and the height above the reference surface *h*, as

$$\phi_{topo} = \frac{4\pi}{\lambda R} \cdot \frac{B_{\perp} \cdot h}{\sin \alpha} \tag{2}$$

ϕ_{defo} : deformation phase due to the deformation *D* in the radar line-of-sight，which can be described as: $\phi_{defo} = \frac{4\pi}{\lambda} D$

ϕ_{orb} : deterministic flat earth phase and the residual phase signal due to orbit indetermination, the flat earth phase can be expressed as a function of the range increment between pixels Δr :

$$\phi_{flat} = \frac{4\pi}{\lambda R} \cdot \frac{B_{\perp} \cdot \Delta r}{\tan \alpha} \tag{3}$$

This residual phase signal forms a linear trend in the interferograms, it can be merged into the atmospheric delay ϕ_{atm} in the computation, because the atmosphere causes a linear trend as well.

ϕ_{atm} : phase related to the atmospheric artifacts

ϕ_{scat} : phase due to a temporal and spatial change in the scatter characteristics of the earth surface between the two observation times

ϕ_{noise} : phase degradation factors, caused by e.g., thermal noise, coregistration noise and interpolation noise.

Generally the deformation can be classified into linear and non-linear component, consequently there are linear and non-linear terms in deformation phase ϕ_{defo} :

$$\phi_{defo} = \phi_{linear} + \phi_{non-linear} = \frac{4\pi}{\lambda}(D_{linear} + D_{non-linear}) = \frac{4\pi}{\lambda} \cdot v \cdot T + \frac{4\pi}{\lambda} \cdot D_{non-linear} \tag{4}$$

where

ϕ_{linear} : phase term of linear deformation D_{linear}

$\phi_{non-linear}$: phase term of non-linear deformation $D_{non-linear}$

v : deformation velocity

T: temporal baseline between two SAR acquisitions

By removing the flat earth phase and the topographic reference phase using differential InSAR technique, we obtain the differential phase:

$$\phi_{dif} = \phi_{topoerror} + \phi_{defo} + \phi_{atm} + \phi_{scat} + \phi_{noise} \tag{5}$$

After removal of the topographic reference phase, a residual topographic phase is left due to the inaccuracy of the DEM:

$$\phi_{topo-error} = \frac{4\pi}{\lambda R} \cdot \frac{B_{\perp} \cdot \Delta h}{\sin \alpha} \tag{6}$$

where Δh is the height error of the DEM used in the DInSAR processing.

III. DATA PROCESSING AND RESULTS ANALYSIS

The permanent scatterers processing technique is validated by using the ERS-1 and ERS-2 SAR data covering the city of Las Vegas of the United States from April, 1991 to February, 2002, 50 orbits SAR data (track356, frame2871) were collected, in order to select the master images of the algorithm, we plot the baselines and the time span of every acquisition in the data set in Figure1, the orbit 09228 is selected as the master image.

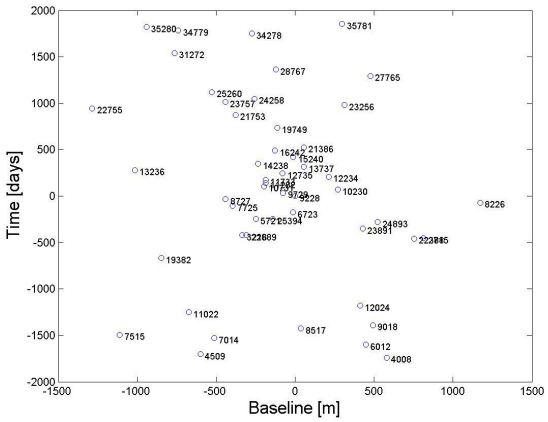

Figure1. Spatial and temporal baseline plot of the Las Vegas InSAR data set, from this plot we choose the orbit 09228 as the master image of the permanent scatterers processing technique

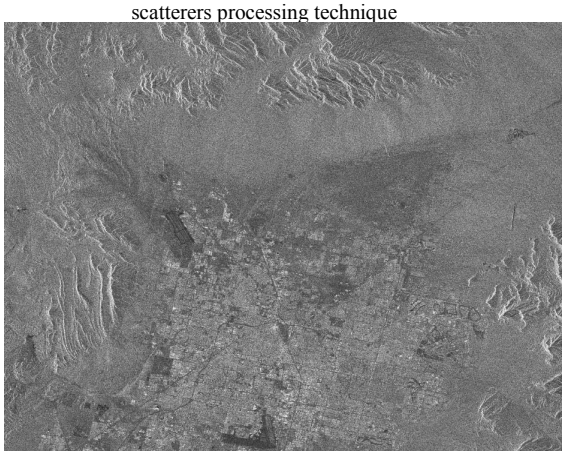

Figure2 Amplitude SAR image of Las Vegas（orbit:09228, track:356, frame:2871）

Figure2 shows the amplitude SAR image of Las Vegas city. which has been despeckled for the purpose of clear visualization.

After the calibration of SAR data stack, 49 interferograms are generated with the same master of 0rbit 09228, the flat earth phases are substracted. In 49 interferograms, only half of them have nice fringe maps, which means higher coherence of the interferometric pairs. Using the amplitude dispersion criteria, by setting the threshold of amplitude dispersion to 0.25, we select 1476371 points as permanent scatterer candidates. The phase gradients are formed by Delaunay triangulation as depicted also in Figure3.

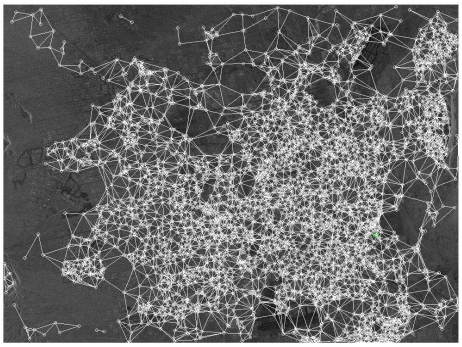

Figure3. Selected permanent scatterer candidates using amplitude dispersion of 0.25 and Delaunay triangulations

By using two dimension periodogram technique, the DEM (because the differential phase is not used in our processing, the DEM here is a relative elevation) and linear deformation of the edges between PSCs are estimated. After estimation, the original phase values are corrected for the DEM and linear deformation. Then the ensemble phase coherence is calculated after the subtraction of DEM and linear deformation phase, the ensemble phase coherence is used as data weights in the phase unwrapping of the PSCs on sparse grid. We set a threshold of the ensemble phase coherence as 0.6, if the ensemble phase coherence is smaller than the threshold, the edge is excluded.

We estimate the atmospheric phase of the master image by averaging, and subtract it from the unwrapped phases, then a low pass filtering is implemented to the time series to remove the non-linear deformation and get the atmospheric phase of every slave images.

Once we get the atmospheric phase of every PSC, a kriging interpolation can be used to derive the atmospheric phase screen of every acquisitions, from which we can see the changing of atmospheric conditions in the time interval between two acquisitions, but it is too coarse and without meteorologic material to testify them, which still need deep investigation.

After removing the APS of every acquisitions, again we select the permanent scatterers, form PS network, and estimate the DEM and linear deformation of the permanent scatterers by 2D periodogram technique, the results are shown in Figure4 and Figure5.

IV. CONCLUSIONS

In this paper, we test the permanent scatterers algorithm by time series SAR data in Las Vegas, results of linear deformation and relative DEM of selected permanent scatterers are achieved. The next step of our research is to validate this algorithm by the data set in cities of China as Beijng, Tianjin and Shanghai.

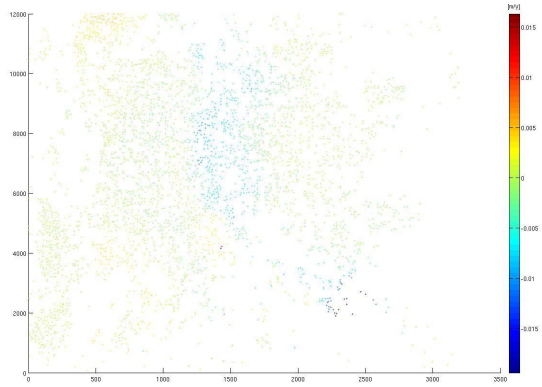

Figure4. Linear deformation velocity of permanent scatterers

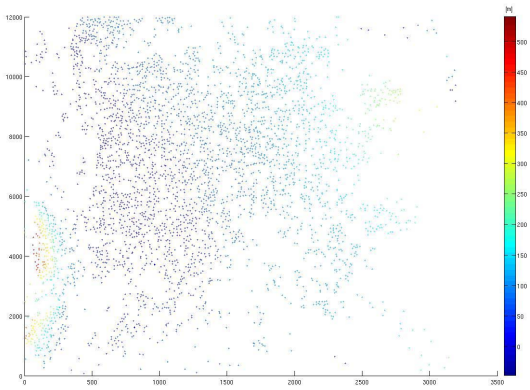

Figure5. Relative DEM of permanent scatterers

REFERENCES

[1] Ferretti, A., C Prati, and F Rocca, "Nonlinear subsidence rate estimation using permanent scatterers in differential SAR interferometry", IEEE Transactions on Geoscience and Remote Sensing, vol. 38(5), pp. 2202-2212, September 2000.

[2] Ferretti, A., C Prati, and F Rocca, "Permanent scatterers in SAR interferometry", IEEE Transactions on Geoscience and Remote Sensing, vol. 39(1), pp. 8-20, January 2001.

[3] National Research Council, "Mitigating losses from land subsidence in the United States", Washington, D.C., National Academy Press, p. 58, 1991.

[4] Gabriel, A.K. RM Goldstein, and H A Zebker, "Mapping small elevation changes over large areas: differential radar interferometry", Journal of Geophysical Research, vol. 94(B7), pp. 9183-9191, July-10 1989.

[5] Hanssen, R.F., "Radar Interferometry: Data Interpretation and Error Analysis", Kluwer Academic Publishers, Dordrecht, 2001.

[6] Amelung, F., S Jónssen, H Zebker, and P Segall, "Widespread uplift and trap door faulting on Galápagos volcanoes observed with radar interferometry", Nature, vol. 407(6807), pp. 993-996, October-26 2000.